MJSAT

*Malaysian Journal of Science and Advanced Technology*

journal homepage: https://mjsat.com.my/

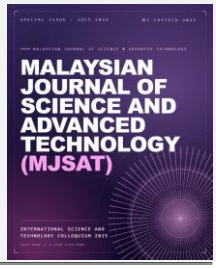


# Effect of LiTFSI Incorporation on the Structural, Electrical, Mechanical and Morphological Properties of PMMA-DES Electrolyte Films

Nurin Afiqah Mohd Azli[1], Siti Zulaikha Mohd Yusof*[1], and Nurul Hanis Syamimi Abdul Fattah[1]

[1]*Faculty of Applied Science, Universiti Teknologi Mara Cawangan Perlis, Kampus Arau, 02600, Arau, Malaysia.*

**KEYWORDS**

*Solid polymer electrolyte*
*Poly methy methacrylate*
*Lithium bis(trifluoromethane-sulfonyl)imide*
*Ionic conductivity*

**ARTICLE HISTORY**

*Received 22 November 2025*
*Available online 21 August 2026*

**ABSTRACT**

Solid polymer electrolytes (SPEs) are lightweight, flexible alternatives to liquid electrolytes for lithium-ion batteries, while the limited ionic conductivity and other factors related to morphological stability limit their applicability. In this study, the results were successfully obtained with PMMA-based electrolytes when modified with lithium bis(trifluoromethanesulfonyl)imide (LiTFSI) and a choline chloride/1,3-propanediol deep eutectic solvent (DES). PMMA-LiTFSI-DES thin films were solvent cast and characterized using Fourier transform infrared spectroscopy (FTIR), electrochemical impedance spectroscopy (EIS), tensile testing, and optical microscopy (OM). FTIR demonstrated strong interactions between the polymer and the salt, with a peak intensity of 98.99% with respect to the absorbance peak for the PMMA10$_{DES}$ sample. EIS showed a significant increase in conductivity from $1.61 \times 10^{-8}$ S cm$^{-1}$ without LiTFSI to $1.76 \times 10^{-6}$ S cm$^{-1}$ with 10 wt.% of LiTFSI content. Tensile testing indicated that PMMA10$_{DES}$ had the highest tensile strength (6.3 MPa) and Young's modulus (4513 MPa) when comparing separate films. For morphological study, OM indicated that the DES artificially induced heterogeneous domains and that 10 wt.% LiTFSI allowed a uniformly homogeneous microstructure that was indicative of only very minimal phase separation. Results indicate that the unique combination of effects from combining both DES and low concentration of LiTFSI improved ionic conductivity, mechanical strength, and morphological stability. Therefore, PMMA-based SPEs show exceptional promise for the advancement of solid-state batteries for next generation applications.



## 1. INTRODUCTION

Fenton et al (1973) were the first to report on polymer electrolytes, and large-scale potential was highlighted in the early 1980s [1]. In General, polymer electrolytes can be described as membranes with transport properties of conventional liquid ionic solutions. Membranes are consisted of polymer matrices, have high molecular weight, and absorb dissolved ions [2]. Polymer electrolytes come in three state which are solid polymer electrolyte (SPE), liquid electrolytes (LE), and gel polymer electrolytes (GPE). SPEs are solvent-free electrolytes as the positively charged cations and negatively charged anions are weakly bonded and easily transported [2].

At moderate temperatures, the material is thermally stable and remains intact, and it acts as a ceramic ionic conductor at temperatures above a defined threshold, but it is also brittle under pressure.

This research highlights PMMA as a potential polymer host due to its excellent properties. The improvements to mechanical pliability and conductivity were due to the addition of DES to the polymer matrix, along with the addition of LiTFSI as the salt for lithium-ion transport to increase ionic conductivity. Finally, it highlighted recent advances, noted issues with improving polymer-salt interactions and proposed areas for future work to develop high performance polymer electrolytes for energy storage applications in general.

*Corresponding author:
E-mail address: Siti Zulaikha Mohd Yusof < sitizulaikhamy@uitm.edu.my >.
https://doi.org/10.56532/mjsat.v6iS1.791

The SPEs belong to a kind of polymer electrolyte which has a complete solid-state composition in nature, offering ionic conduction in an electrochemical device. It is different from liquid-based and gel-based SPEs, which, in their basic nature, contain a matrix of selected polymers combined with salt to enhance the conduction of ions. Apart from acting as an ionic conductor, SPEs also act as a separator between electrolyte and electrode in cells or batteries, and thus there is no need to use inert porous spacers. They also function as binders, providing electrical contact with electrodes, and hence there is no need for a high temperature process, which is required in liquid electrolytes [1]. It was believed until recently [3] that the fast-ion transport in SPEs was chiefly due to an amorphous phase in the polymeric host. It had been assumed that a greater proportion of amorphous results in enhanced ionic conduction in SPEs. The first representative of a "dry solid" polymer electrolyte was poly(ethylene oxide) (PEO) based systems and their conductivities at ambient temperature were very low, around $10^{-8}$ S $cm^{-1}$ [4].

Despite extensive studies on polymer electrolytes incorporating ionic liquids or varying plasticizer contents, the effect of lithium salt concentration in DES–plasticized PMMA electrolytes remains insufficiently explored. Systematic investigations on LiTFSI-based DES electrolytes are limited. However, it is crucial to highlight key electrolyte properties including viscosity, ionic conductivity and electrochemical stability are strongly influenced by the LiTFSI mole fraction [23]. Therefore, this work aims to investigate the effect of LiTFSI concentration on the structural, electrical, mechanical, and morphological properties of PMMA–DES electrolyte films. The findings provide clearer insight into polymer–DES-salt interactions and their impact on ionic transport and material performance.

The morphology of the polymer will be affected due to the DES shares similar properties like Ionic Liquid (IL), which restricts hydrogen bonding due to large structure of IL that occupies space between PMMA chains during polymerisation [13]. This localized plasticizing effect due to the interaction of LiTFSI doped into PMMA electrolyte system, reduces the free ions available for polymer matrix. The modification of PMMA-DES is created through LiTFSI doping to avoid being brittle. In return, the modification increases lithium ions mobility and the strength of the composite. Hence, the resultant polymer electrolyte is suitable for energy storage applications because of its enhanced conductivity and mechanical property.

## 2. METHODOLOGY

### *2.1 Chemicals and Materials*

In this work, PMMA (Mw = 120,000) has been used as a polymer (host) matrix and LiTFSI as a doping salt. These were purchased from Sigma-Aldrich. Meanwhile, dichloromethane (DCM) was used as the solvent and DES which is choline chloride 1,3-propenediol acts as plasticizer. Both were prepared in the preliminary study.

### *2.2 Preparations of PMMA-LiTFSI-DES films*

Preparation of the PMMA-doped LiTFSI solid polymer electrolyte system involves several steps to ensure LiTFSI is well dispersed within the PMMA matrix. The solution casting technique was used for the preparation of polymer electrolyte thin films. This process generally occurs in a suitable solvent that can dissolve both the polymer and the dopant. Moreover, this technique allows for the addition of other components, such as plasticizers, ceramic fillers, or nanoparticles, into the polymer matrix. Such additives can be mixed into the casting solution to alter properties like ionic conductivity, thermal stability, and mechanical strength. Accurately weighted amounts of PMMA, LiTFSI and DES depend on the required composition

Table 1 summarizes the quantities of LiTFSI used to prepare the PMMA-LiTFSI-DES SPEs at three different salt concentrations (10, 30, and 50 wt.%). For each sample, 1.0 g of PMMA and 0.2 g of DES (20 wt.% relative to PMMA) were used. PMMA and DES were dissolved in 20 mL of DCM under continuous magnetic stirring at room temperature until a clear and homogenous solution was obtained. The DES was incorporated as a plasticizing agent to enhance ionic mobility and improve film flexibility, consistent with previously reported polymer electrolyte systems [6]. This fixed amount was used as a plasticizing additive to enhance polymer chain flexibility and promote ionic mobility. This concentration was selected as it provides sufficient plasticization to improve ion transport while maintaining the mechanical stability and free-standing nature of the electrolyte film. LiTFSI was subsequently added to the PMMA–DES solution and stirred further at room temperature to ensure complete dissolution and homogeneous mixing. The resulting homogeneous solution was cast onto a clean Petri dish, and the film thickness was controlled by the volume of solution spread over the substrate. The cast films were dried in a fume hood at room temperature for 24 h to remove residual DCM. After drying, the films were stored in a desiccator until further characterization to prevent moisture absorption and ensure complete solvent evaporation, yielding solid polymer electrolyte films composed of PMMA, LiTFSI, and DES.

**Table 1.** Composition of PMMA-LiTFSI-DES Polymer Electrolyte System

| Designation | PMMA (g) | LiTFSI (wt.%) | LiTFSI(g) |
|---|---|---|---|
| PMMA0 | 1.0 | 0 | 0.0 |
| PMMA0DES | 1.0 | 0 | 0.0 |
| PMMA10DES | 1.0 | 10 | 0.1 |
| PMMA30DES | 1.0 | 30 | 0.3 |
| PMMA50DES | 1.0 | 50 | 0.5 |

## 3. CHARACTERIZATIONS METHODS

### *3.1 Fourier Transforms Infrared Spectroscopy (FTIR)*

FTIR analysis was conducted with an Attenuated Total Reflectance (ATR)-equipped Thermo Fisher Scientific Nicolet iS 10 to study molecular interactions in the PMMA-DES-LiTFSI system. Spectra were obtained in transmittance mode between 4000 and 600 $cm^{-1}$ with a resolution of 2 $cm^{-1}$ and five scans at room temperature. Samples (1 cm x 1 cm) were applied directly on the ATR crystal. This method was used to ascertain any coordination between lithium ions and carbonyls of PMMA and potential hydrogen bonding or ionic interactions that were added by DES.

### 3.2 Electrochemical Impedance Spectroscopy (EIS)

Ionic conductivity of the PMMA-DES-LiTFSI films was evaluated using a HIOKI 35232-01 LCR meter over a frequency range of 100 Hz to 1 MHz at room temperature. Film samples (2.5 × 2.5 cm) were placed between stainless steel blocking electrodes, and thickness was measured with a micrometer screw gauge, averaging five readings. The impedance data were used to determine the bulk resistance ($R_b$), from which the ionic conductivity ($\sigma$) was calculated using:

$$\sigma = \frac{R_b A}{L} \quad (1)$$

Where $L$ is the film thickness (cm), $A$ is the electrode-electrolyte contact area (cm²), and $Rb$ is the bulk resistance (ohms). The composition with the highest conductivity was studied to assess the effect of DES on the ionic transport since its addition is known to increase the segmental mobility and establish more efficient pathways of ionic transport.

### 3.3 Tensile Test

The test samples were prepared in dimensions of 1 cm in width and 7 cm in length. Note that due of its extreme brittleness, pure PMMA was not utilised in tensile testing. The thin films were measured five times for accuracy using micrometre screw gauge. In this study, mechanical properties of the thin film samples were evaluated using an Instron Universal Testing Machine (Model 3365, Instron, USA). The crosshead speed was maintained at 10 mm·min⁻¹. From a mechanical standpoint, two important parameters are tensile strength and Young's modulus ($E$). Tensile strength is calculated by dividing the applied force ($F$) by the original cross-sectional area of the film ($A_0$), as shown below:

$$Tensile\ stress = \frac{F}{A_o} \quad (2)$$

Young's modulus ($E$) is called the modulus of elasticity and can be determined by the ratio of the tension stress to the extensional strain of the film. In the other forms, it can be summarized as below:

$$E = \frac{F\, l_o}{A_o\, \Delta l} \quad (3)$$

Where $E$is Young's modulus (Pa), $F$is the applied force (N), $l_0$is the initial length of the object (m), $A_0$is the original cross-sectional area where the force is applied during the test (m²), and $\Delta l$is the change in length of the object before and after testing.

### 3.4 Optical Microscopy (OM)

The morphology of the PMMA-LiTFSI-DES based electrolyte films was examined using an optical microscope (Olympus CX31) to observe surface features. The samples were cut into squares (1 cm × 1 cm) and images were captured at 10x magnification using Dino-Lite Digital Microscope software. These observations provided qualitative insights into the surface texture and general uniformity of the films, without implying quantitative homogeneity.

## 4. Results And Discussion

### 4.1 PMMA-LiTFSI-DES Films

Figure 1 shows the PMMA-LiTFSI-DES thin films successfully obtained for all compositions. The films remained solid at the room temperature and being kept inside the desiccator prior to characterization. A DCM solvent was used to prepare the thin film of PMMA0 (Figure 1(a)), which exhibited transparent and uniform appearance, indicating the PMMA was well dissolved in the solvent. The relatively uniform film appearance suggests that phase separation during casting was minimal, which can be attributed to the good compatibility of PMMA with DCM, a non-polar solvent with a low boiling point [12]. In contrast, the $PMMA0_{DES}$ and $PMMA10_{DES}$ films (Figure 1 (b)-(c)) appeared cloudy, which is likely due to partial precipitation or phase separation of the polymer. DESs contain hydrogen bond donors and acceptors that may crystallize under specific conditions, such as variations in temperature or humidity [6].

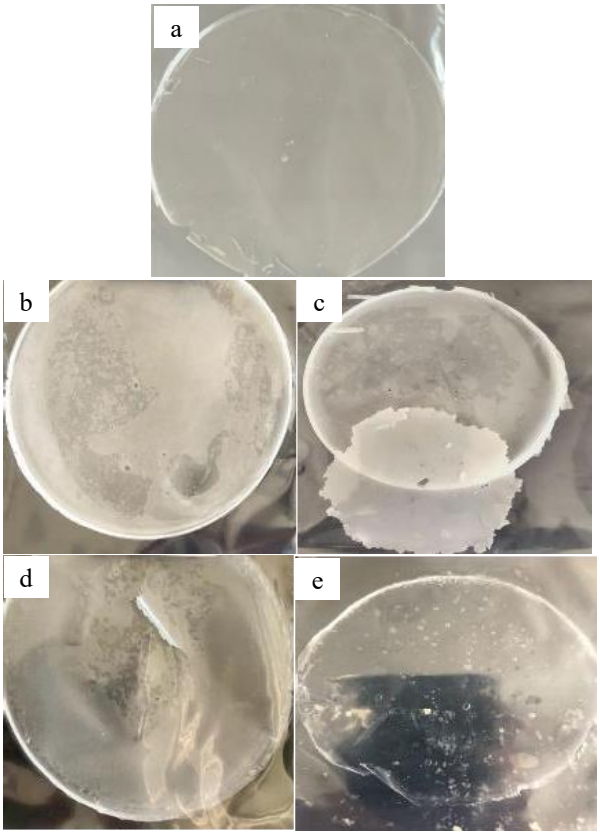


**Fig. 1.** The Photographs of (a) PMMA0, (b) PMMA0DES, (c) PMMA10DES, (d) PMMA30DES, and (e) PMMA50DES

When the DES components start crystallizing during or after casting, this also leads to cloudiness because of scattering of light by crystalline structures. Moreover, the broken PMMA30DES (Figure 1 (d)) was monitored. This may be attributed to internal forces brought about by non-uniform drying or non-compatibility of the polymer and the salt-saturated regions. Thereafter, PMMA50DES (Figure 1 (e)) depicted the apparent thin film with visible cracks and folds. Such brittleness is noticeable in this film since the polymer concentration is large, which causes a dense network hindering

the movement of polymer chains and slowing the exchange of ions [5].

### 4.2 Structural Analysis

Figure 2 indicates the FTIR spectra of PMMA-DES-LiTFSI electrolyte films with different LiTFSI concentrations (0, 10, 30, and 50 wt.%). The typical peaks of PMMA were located at 2947 $cm^{-1}$ (C-H stretching) [14, 15], 1727 $cm^{-1}$ (C=O stretching of ester group) [15], and 747 $cm^{-1}$ ($CH_2$ rocking) [15]. Peaks at 1145 $cm^{-1}$ (C-$SO_2$-N) [16] and 982 $cm^{-1}$ (CO-$CH_3$ rocking) [15] correspond to the presence of LiTFSI and its interaction with the polymer matrix. The increased intensity of the peaks, especially at 1727 $cm^{-1}$ (C=O) and 1145 $cm^{-1}$ (C-$SO_2$-N) with LiTFSI addition indicates coordination of lithium ions with the carbonyl groups of PMMA, as well as interactions between the DES and the polymer backbone. Among the samples, $PMMA10_{DES}$ exhibited the highest peak intensities (average 98.99%), reflecting optimal distribution of LiTFSI and DES within the polymer matrix. This observation agrees with the EIS results, where $PMMA10_{DES}$ exhibited the highest ionic conductivity, indicating that optimal salt dissociation and polymer–ion interactions occur at this composition. At higher salt content (50 wt.%), the peaks broadened and showed reduced intensity, suggesting partial phase separation and limited disruption of polymer ordering. Peak broadening at higher salt loading is commonly attributed to increased structural disorder and overlapping vibrational modes, which may arise from salt clustering and non-uniform ion coordination. Since the DES content was kept constant, the observed changes in molecular interactions, segmental mobility, and amorphous content are primarily due to LiTFSI addition, rather than DES. Although LiTFSI is the main contributor to the conductivity enhancement, DES provides a polar ionic environment that supports ion solvation and coordination within the PMMA matrix. In addition, the DES contains intrinsic ionic species that can contribute to charge transport, which explains the measurable baseline conductivity observed in $PMMA0_{DES}$ even without LiTFSI. These observations are consistent with previous studies [17, 18], where DES was reported to facilitate molecular interactions and improve ionic pathways. Overall, the peak intensities and broadening patterns in $PMMA10_{DES}$ indicate strong interactions among PMMA, LiTFSI, and DES, promoting efficient ion transport.

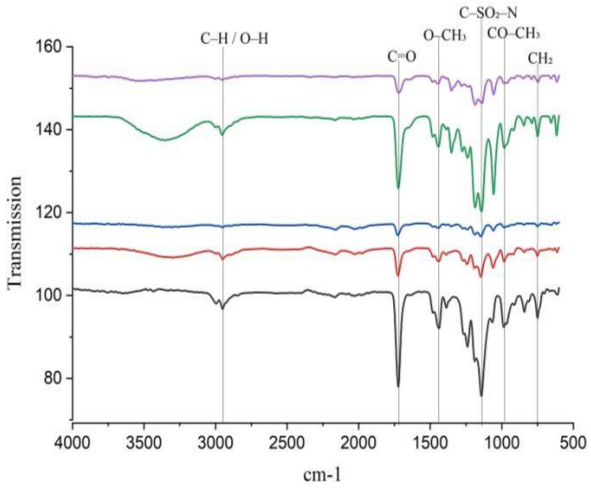


**Fig. 2.** FTIR Spectra of PMMA-DES-LiTFSI Systems

### 4.3 Ionic Conductivity Analysis

Table 2 summarizes the ionic conductivity of the PMMA–DES–LiTFSI electrolyte films. All measurements were performed in triplicate and the average values are reported to ensure reproducibility. A similar PMMA–DES system without lithium salt has been reported to exhibit an ionic conductivity of 2.56 x $10^{-8}$ S·$cm^{-1}$ [13]. In the present work, the DES-containing sample without LiTFSI ($PMMA0_{DES}$) showed a slightly lower ionic conductivity of 1.61 x $10^{-8}$ S·$cm^{-1}$, confirming that the DES provides intrinsic ionic charge carriers, such as choline cations and chloride-based anions, which can facilitate ion transport even in the absence of LiTFSI.

**Table 2**. Ionic Conductivity of PMMA-DES-LiTFSI

| Designation | Bulk Resistance | Ionic Conductivity, $\sigma$ (S $cm^{-1}$ x$10^{-8}$) |
|---|---|---|
| $PMMA0_{DES}$ | 243.00 | 1.61 |
| $PMMA10_{DES}$ | 2.82 | 176 |
| $PMMA30_{DES}$ | 62.00 | 3.22 |
| $PMMA50_{DES}$ | 170.00 | 1.22 |

The slightly lower conductivity obtained in the present work may also be influenced by differences in the solvent used during film casting. The previous study [13] employed tetrahydrofuran (THF), whereas dichloromethane was used in this work. Since DCM has a lower boiling point and evaporates more rapidly, it may lead to a denser film structure with reduced residual solvent and lower free volume, resulting in slightly reduced ion mobility. Nevertheless, the conductivity values remain comparable and within the same order of magnitude.

Upon incorporation of 10 wt.% LiTFSI, the ionic conductivity increased significantly due to the higher concentration of mobile $Li^+$ ions and improved ion transport within the polymer matrix. The use of DCM as a solvent also promotes uniform film formation and effective salt dispersion. Although $PMMA10_{DES}$ exhibited the lowest bulk resistance among all compositions, the absolute $R_b$ values remain relatively high compared to practical battery electrolyte requirements. This is mainly due to the inherently insulating nature of PMMA and the limited concentration of free mobile ions in the current system. Nevertheless, the results clearly demonstrate the important role of LiTFSI concentration in governing ion dissociation and ionic transport.

Figure 3 presents the Nyquist plots (Cole-Cole) for the PMMA-DES-LiTFSI electrolyte films with varying LiTFSI content. All samples show a depressed semicircle at the high frequencies region followed by a spike at the low frequencies region. The semicircle corresponds to the bulk resistance (Rb), while the spike indicates capacitive behavior at the electrode–electrolyte interface, consistent with previously reported trends in polymer–salt systems [19]. Among all compositions, the PMMA10DES sample exhibited the smallest semicircle diameter, corresponding to the lowest bulk resistance (Rb = 2.82 × 104 Ω) and, consequently, the highest ionic conductivity (1.76 × $10^{-6}$ S $cm^{-1}$). In accordance with previous findings, this enhancement is ascribed to the efficient dissociation of LiTFSI, which raises the quantity of free ions, as well as the enhanced segmental motion of the polymer chains made possible by the interaction between $Li^+$ and the polar functional groups of PMMA–DES [19].

However, at higher salt concentrations (30 wt.% and 50 wt.%), the ionic conductivity decreases $3.22 \times 10^{-8}$ S cm$^{-1}$ and $1.22 \times 10^{-8}$ S cm$^{-1}$, respectively. This reduction is likely due to the formation of ion aggregates or ion pairs at high salt content, where $Li^+$ and $TFSI^-$ form neutral clusters that do not contribute to ionic transport [19]. Moreover, excessive salt content may increase the viscosity and restrict polymer chain mobility, reducing the amorphous phase that is essential for efficient ion transport.

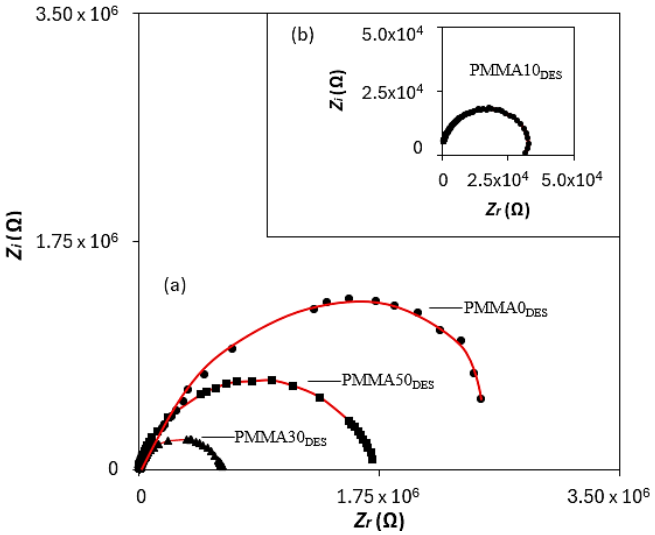


**Fig. 3**. Nyquist Plots for (a) PMMA0DES, (b) PMMA10DES, (c) PMMA30DES and (d) PMMA50DES

### *4.4 Mechanical Analysis*

The tensile test was carried out to study the mechanical behaviour of the polymer electrolyte composites made with PMMA-DES and varying LiTFSI in the range of 0% - 50%. PMMA-DCM can be neglected in this test due to the brittleness of the thin film. The tensile stress–strain curve for the PMMA0DES (a) film can be seen in Figure 4. The curve shows a typical linear elastic behaviour until it reaches the maximum tensile stress, followed by brittle failure with minimal plastic deformation [24]. The maximum tensile stress occurs at ~1.1 MPa with a strain at break of ~0.00045 (0.045%). The linear portion of the curve shows that the material behaves elastically at low deformation and is fulfilling Hooke's Law. The steep slope of the straight part shows that the Young's modulus is high at 2706 MPa, meaning the polymer matrix is rigid and stiff.

According to Hooke's Law, the curve's linear beginning denotes an elastic state at low deformation. The slope's steepness suggests that a rigid and stiff polymer matrix, or PMMA, is linked to a high Young's modulus. This is also in line with the definition of a typical PMMA-based system [7]. The sharp stress drop after the yield point indicates that the film has a total failure without much elongation. This fact indicates that the DES mechanical response is inadequate to perform as an efficient plasticizer in the PMMA matrix [6]. DES is known to decrease rigidity by disturbing the packing of polymer chains [6], but clearly in this case the available amount is not sufficient to break the strong van der Waals and dipole interactions between PMMA chains.

The tensile stress–strain response of the PMMA10DES (b) is observed in Figure 4. The curve shows a linear elastic region, followed by a peak stress of approximately 6.3 MPa at a magnitude of strain of approximately 0.0021. The Young's modulus obtained from this graph is the highest which is 4513 MPa. The stress then drops sharply, suggesting brittle fracture is occurring with very low plastic deformation. The moderate tensile strength indicates that incorporation of DES and LiTFSI has not caused any noticeable loss in mechanical integrity. DES has been shown to act as a plasticizing agent, reducing intermolecular interactions of the polymer, and increasing flexibility to some degree [6]. Tensile stress–strain curve of the PMMA30DES (c) in Figure 4 shows that the stress continues to increase with strain until it reaches a maximum at 1.9 MPa at a strain of ~0.0007 and Young's modulus at 3314 MPa. The stress then decreases gradually prior to failure, showing that the material is beginning to soften or fail based upon the stress values. The tensile strength and strain at break of PMMA30DES is lower than the PMMA10DES, providing further evidence of mechanical integrity loss with increasing of LiTFSI. The decrease in tensile properties may be due to the increased LiTFSI content which likely increases ionic content in the polymer matrix and weakens the cohesive forces between PMMA chains while introducing structural heterogeneities.

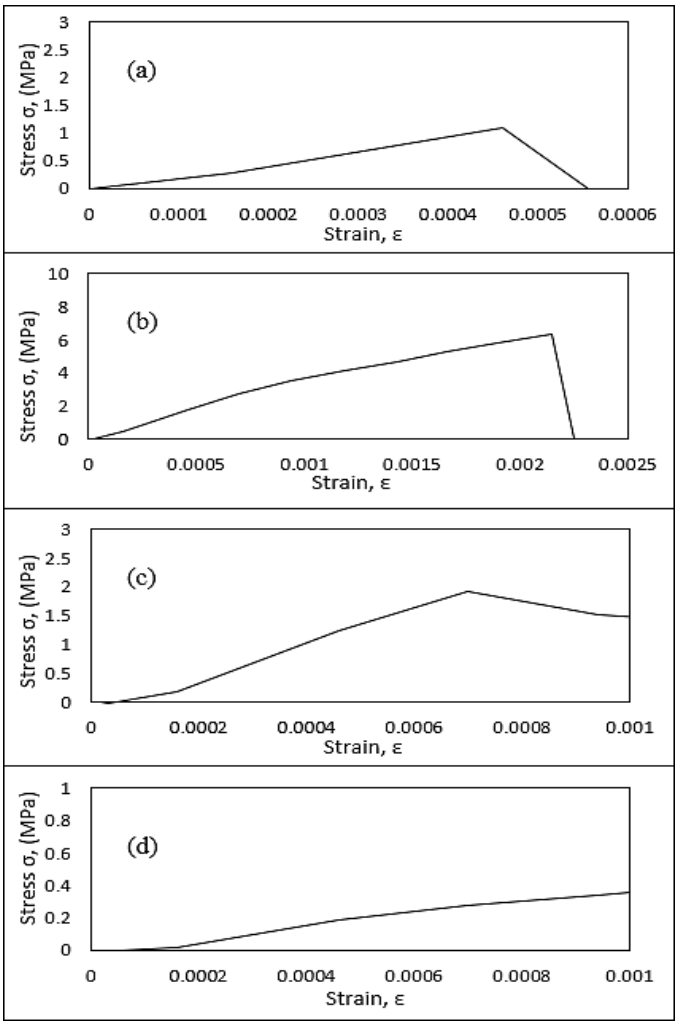


**Fig. 4.** Stress-strain Curve for (a) PMMA0DES, (b) PMMA10DES, (c) PMMA30DES and (d) PMMA50DES

Elevated salt loading can disrupt the polymer's network for the polymer and can decrease its mechanical stiffness and load bearing properties [2], [7]. While LiTFSI maintains good ionic conductivity at high concentrations, LiTFSI will act as a plasticizer, further decreasing crystallinity and modulus [8]. Furthermore, high concentrations of salts likely will result in phase separation or agglomeration of salts [9]. The PMMA50DES (d) sample tensile stress-strain curve is illustrated in Figure 4.

The stress response is demonstrated to gradually increase with strain to an ultimate value of only ~0.34 MPa at a strain of 0.001 with no obvious indication of material fracture within the range measured and lowest Young's modulus at 315 MPa. The low stress value and lack of a distinct point of failure suggest that the material has become soft and mechanically weak with excessive salt. The results of the tensile stress and Young's modulus tests as shown in Table 3 indicated that the presence of different amounts of deep eutectic solvent (DES) influenced the mechanical properties of PMMA. The addition of 10% DES increased tensile stress to 6.3 MPa and Young's modulus to 4513.53 MPa, indicating improved intermolecular interaction and later improved reinforcement of the polymer network at this level of composition. However, the higher amounts of DES (30% and 50%) revealed a decrease in tensile stress (1.9 MPa and 0.34 MPa), especially in the case of the PMMA50DES modulus, which reflected the lowest stiffness (315.21 MPa). The results thus suggest that while moderate DES incorporation can improve mechanical strength and rigidity, it can also plasticize the material or compromise integral structure if excessive amounts are added.

**Table 3.** Comparison of Thin Films in Tensile Stress and Young's Modulus

| Samples | Tensile stress, σ (MPa) | Young's modulus, E (MPa) |
|---|---|---|
| $PMMA0_{DES}$ | 1.1 | 2706.00 |
| $PMMA10_{DES}$ | 6.3 | 4513.53 |
| $PMMA30_{DES}$ | 1.9 | 3314.88 |
| $PMMA50_{DES}$ | 0.34 | 315.21 |

*4.5 Morphological Analysis*

All samples were characterized with optical microscopy (OM) and at the 10x magnification. Figure 5(a–e) depicted the morphological structures of PMMA0, PMMA0DES, PMMA10DES, PMMA30DES and PMMA50DES electrolyte samples, respectively. The optical microscopy of a solution containing 1.0 g of PMMA dissolved in 20 ml of DCM in Figure 5 (a) displayed a microstructure with discrete spherical droplets of various diameters in the field of view, suggesting the microphase separation that occurred during DCM evaporation and led to the nucleation and growth of PMMA microspheres. The polydispersity from submicron to several micrometres in diameter indicates heterogeneous nucleation and growth.

The optical micrographs of the PMMA-DES composite film in Figure 5 (b), showed a heterogeneous microstructure of dispersed spherical domains in a continuous polymer matrix, which showed partial phase separation, common when hydrophilic DESs, such as choline chloride 1,3-propanediol, are incorporated into PMMA (a hydrophobic polymer). The casting solvent, DCM, evaporates quickly which contributes to kinetic trapping of the DES domains and results in frozen-in phase-separated structures [10]. This behaviour results from the polarity mismatch between the two phases, which hinders the formation of a fully homogeneous blend [11].

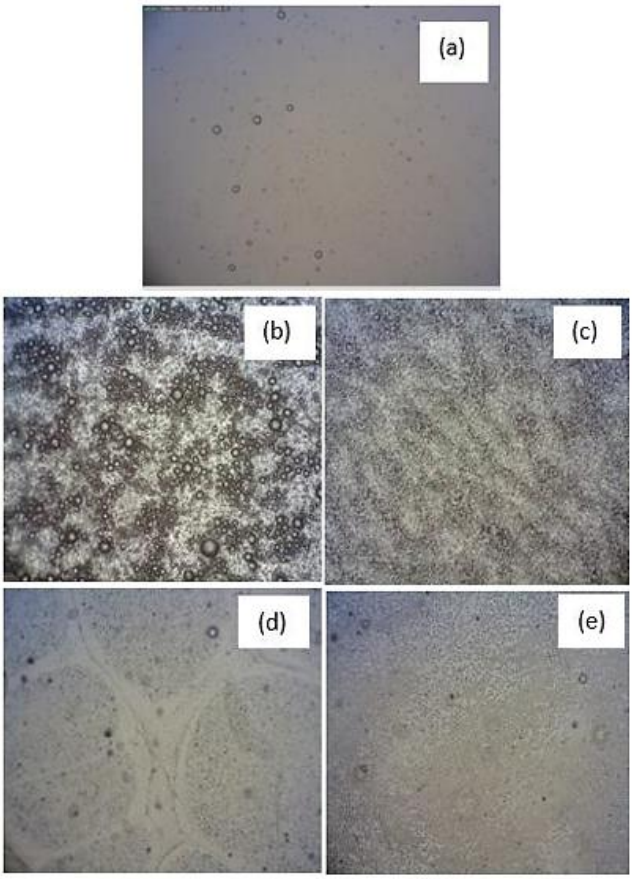


**Fig. 5.** OM Micrographs of PMMA–DES–LiTFSI electrolyte films (a–e: PMMA0, $PMMA0_{DES}$, $PMMA10_{DES}$, $PMMA30_{DES}$, PMMA50DES)

Next, Figure 5 (c) showed the micrograph of PMMA10DES indicated more uniform and finer dispersion pattern. The reduction in droplet size and increased uniformity is because the presence of LiTFSI contributes to improved dispersion. The relatively even distributed spherical features suggest enhanced compatibility among components. The LiTFSI is not only acts as an ion source but also modifies polymer morphology by altering phase behaviour [10]. The DES serve as a plasticizing and coordinating medium for LiTFSI at once stabilize the dispersion. Figure 5 (d) showed the sample exhibits the formation of larger and more defined regions observed under the microscope. The increasing of LiTFSI salt in polymer may lead to ion clustering as lithium salt concentrations exceed the coordination capacity of the host matrix. The last Figure 5 (e) showed a high density of microdomains and distinct phase boundaries. The increased salt content likely exceeds the coordination capacity of the PMMA matrix and the DES, resulting in the formation of ionic aggregates. This behaviour is consistent with previous findings, where high concentrations lithium salts such as LiTFSI in polymer matrices lead to ion pair.

## 5. CONCLUSION

A new solid polymer electrolyte (SPE) based on PMMA, LiTFSI, and DES was successfully developed using the solution casting method. Electrochemical impedance spectroscopy showed that the $PMMA10_{DES}$ sample achieved the highest ionic conductivity of $1.76 \times 10^{-6}$ S cm$^{-1}$ at 10 wt.% LiTFSI, attributed to an optimal balance between free ion availability and reduced ion aggregation. FTIR analysis confirmed strong interactions among PMMA, LiTFSI, and DES, as indicated by the broadening and reduced intensity of the carbonyl (C=O) and ether (C–O–C) peaks. Optical microscopy further revealed that PMMA10DES exhibited the most uniform morphology with fine spherical dispersed domains, while higher LiTFSI loadings induced phase separation and ionic aggregation. From a mechanical standpoint, $PMMA10_{DES}$ showed the highest tensile strength (6.3 MPa) and Young's modulus (4513 MPa), although increased salt concentration reduced strength and stiffness while improving elongation due to polymer plasticization. Overall, $PMMA10_{DES}$ demonstrated the most favorable combination of morphology, mechanical integrity, and ionic conductivity, establishing it as a promising candidate for stable solid-state electrochemical devices.

## REFERENCES


[1] Ngai, K. S., Ramesh, S., Ramesh, K., & Juan, J. C. (2016). A review of polymer electrolytes: fundamental, approaches and applications. In *Ionics* (Vol. 22, Issue 8, pp. 1259– 1279). Institute for Ionics. doi: https://doi.org/10.1007/s11581-016-1756-4

[2] Ramesh, S., & Liew, C. (2012). Development and investigation on PMMA–PVC blend-based solid polymer electrolytes with LiTFSI as dopant salt. *Polymer Bulletin*, *70*(4), 1277–1288. doi: https://doi.org/10.1007/s00289-012-0851-6

[3] Agrawal, R. C., & Pandey, G. P. (2008). Solid polymer electrolytes: Materials designing and all-solid-state battery applications: An overview. *Journal of Physics D: Applied Physics*, *41*(22). doi: https://doi.org/10.1088/0022-3727/41/22/223001

[4] Stephan, A. M. (2006). Review on gel polymer electrolytes for lithium batteries. In *European Polymer Journal* (Vol. 42, Issue 1, pp. 21–42). doi: https://doi.org/10.1016/j.eurpolymj.2005.09.017

[5] Wang, X., Zhang, Z., Qin, J., Shi, W., Liu, Y., Gao, H., & Mao, Y. (2017). Enhanced photovoltaic performance of perovskite solar cells based on ER-YB co-doped TIO2 nanorod arrays. *Electrochimica Acta*, *245*, 839–845. doi: https://doi.org/10.1016/j.electacta.2017.06.032

[6] Smith, E. L., Abbott, A. P., & Ryder, K. S. (2014). Deep Eutectic Solvents (DESS) and their applications. *Chemical Reviews*, *114*(21), 11060–11082. doi: https://doi.org/10.1021/cr300162p

[7] Zhao, Y., Liu, Q., & Lu, Y. (2020). Structural tuning of polymer electrolytes: Trade-off between mechanical strength and ionic conductivity. *Journal of Materials Chemistry A*, 8(4), 1865–1883.

[8] Wang, Y., Zhang, Z., Li, Z., & Xu, X. (2015). Enhancing mechanical and electrochemical performance of PMMA- based solid polymer electrolyte using PEO as a copolymer. *Electrochimica Acta*, 173, 498–505.

[9] Rajendran, S., Uma, T., & Kannan, R. (2002). Investigations on the effect of plasticizer in PMMA based polymer electrolyte. *Materials Letters*, 57(2), 317–320.

[10] Zhang, Q., De Oliveira Vigier, K., Royer, S., & Jérôme, F. (2012). Deep eutectic solvents: syntheses, properties and applications. *Chemical Society Reviews*, *41*(21), 7108. doi: https://doi.org/10.1039/c2cs35178a

[11] Corrigan, N., Jung, K., Moad, G., Hawker, C. J., Matyjaszewski, K., & Boyer, C. (2020). Reversible- deactivation radical polymerization (Controlled/living radical polymerization): From discovery to materials design and applications. *Progress in Polymer Science*, *111*, 101311. doi: https://doi.org/10.1016/j.progpolymsci.2020.101311

[12] Ibrahim, S., Yusof, N., & Hashim, N. (2019). *Effect of solvent evaporation rate on morphology and performance of PMMA thin films*. Journal of Applied Polymer Science, 136(31), 47892.

[13] Latif, F. A., Zailani, N. a. M., Nazir, K., Yusof, R., Ghani, F. S. A., Ishak, M. a. M., & Zamri, S. F. M. (2023). Effect of the incorporation of choline chloride-based deep eutectic solvent on the flexibility of poly(methyl methacrylate) films. *Journal of Sustainability Science and Management*, *18*(12), 28–42. doi: https://doi.org/10.46754/jssm.2023.12.004

[14] Szilasi, S., Huszank, R., Szikra, D., Váczi, T., Rajta, I., & Nagy, I. (2011). Chemical changes in PMMA as a function of depth due to proton beam irradiation. *Materials Chemistry and Physics*, *130*(1–2), 702–707. doi: https://doi.org/10.1016/j.matchemphys.2011.07.048

[15] Shafie, M. H., Yusof, R., & Gan, C. (2019). Synthesis of citric acid monohydrate-choline chloride based deep eutectic solvents (DES) and characterization of their physicochemical properties. *Journal of Molecular Liquids*, *288*, 111081. doi: https://doi.org/10.1016/j.molliq.2019.111081

[16] Kumar, R., Sharma, J. P., & Sekhon, S. (2005). FTIR study of ion dissociation in PMMA based gel electrolytes containing ammonium triflate: Role of dielectric constant of solvent. *European Polymer Journal*, *41*(11), 2718– 2725. doi: https://doi.org/10.1016/j.eurpolymj.2005.05.010

[17] Yeow, A. T., Chan, M. K., Ong, C. S., & Ho, K. C. (2024). Effects of hydrogen bond donors on PVDF membrane modification using choline chloride-based deep eutectic solvents. *Journal of Industrial and Engineering Chemistry*, *139*, 514–524. doi: https://doi.org/10.1016/j.jiec.2024.05.028

[18] Andrews, W. T., Liebig, A., Cook, J., Marsh, P., Ciocanel, C., Lindberg, G. E., & Browder, C. C. (2018). Development of a PEO-based lithium-ion conductive epoxy resin polymer electrolyte. *Solid State Ionics*, *326*, 150–158. doi: https://doi.org/10.1016/j.ssi.2018.09.013

[19] Mazuki, N., Kufian, M., Saari, M. M., & Samsudin, A. (2023). Influencing of [EDIMP]TFSI in PMMA-PLA doped LiTFSI based hybrid gel polymer electrolyte on the variation in crystallinity phase and ionic conduction properties. *Journal of Non-Crystalline Solids*, *621*, 122634. doi: https://doi.org/10.1016/j.jnoncrysol.2023.122634

[20] Yang, N. (2014). Dichloromethane. In *Elsevier eBooks* (pp. 99–101). doi: https://doi.org/10.1016/B978-0-12-386454-3.01218-5

[21] Abbott, A. P., Boothby, D., Capper, G., Davies, D. L., & Rasheed, R. K. (2004). Deep Eutectic Solvents Formed between Choline Chloride and Carboxylic Acids: Versatile Alternatives to Ionic Liquids. *Journal of the American Chemical Society*, *126*(29), 9142–9147. doi: https://doi.org/10.1021/ja048266j

[22] Aoyagi, H., Okamura, M., Fukunishi, M., Hikichi, S., & Matsumoto, F. (2024). Generation of superoxide ions in the electrochemical reduction of molecular oxygen in concentrated lithium bis(trifluoromethanesulfonyl)imide aqueous solutions. *Electrochimica Acta*, 145228. doi: https://doi.org/10.1016/j.electacta.2024.145228

[23] Dinh, T. T. A., Huynh, T. T. K., Le, L. T. M., Truong, T. T. T., Nguyen, O. H., Tran, K. T. T., Tran, M. V., Tran, P. H., Kaveevivitchai, W., & Le, P. M. L. (2020). Deep Eutectic Solvent Based on Lithium Bis[(trifluoromethyl)sulfonyl] Imide (LiTFSI) and 2,2,2-Trifluoroacetamide (TFA) as a Promising Electrolyte for a High Voltage Lithium-Ion Battery with a LiMn2O4 Cathode. *ACS Omega*, *5*(37), 23843–23853. doi: https://doi.org/10.1021/acsomega.0c03099

[24] Ramanathan, S., Lin, Y., Thirumurugan, S., Hu, C., Duann, Y., & Chung, R. (2024). Poly(methyl methacrylate) in Orthopedics: Strategies, Challenges, and Prospects in Bone Tissue Engineering. *Polymers*, *16*(3), 367. doi: https://doi.org/10.3390/polym16030367